



Fermi National Accelerator Laboratory

FERMILAB-Conf-96/132-E

D0

**Preliminary Measurement of the Inclusive Jet and Dijet Cross
Section in $\bar{p}p$ Collisions at $\sqrt{s} = 1.8$ TeV**

Gerald C. Blazey

For the D0 Collaboration

*Fermi National Accelerator Laboratory
P.O. Box 500, Batavia, Illinois 60510*

June 1996

Presented at the *XXXIst Rencontres de Moriond QCD and High Energy Hadronic Interactions*,
Les Arcs, France, March 23-30, 1996

Disclaimer

This report was prepared as an account of work sponsored by an agency of the United States Government. Neither the United States Government nor any agency thereof, nor any of their employees, makes any warranty, expressed or implied, or assumes any legal liability or responsibility for the accuracy, completeness, or usefulness of any information, apparatus, product, or process disclosed, or represents that its use would not infringe privately owned rights. Reference herein to any specific commercial product, process, or service by trade name, trademark, manufacturer, or otherwise, does not necessarily constitute or imply its endorsement, recommendation, or favoring by the United States Government or any agency thereof. The views and opinions of authors expressed herein do not necessarily state or reflect those of the United States Government or any agency thereof.

PRELIMINARY MEASUREMENT OF THE INCLUSIVE JET AND DIJET
CROSS SECTION IN $\bar{p}p$ COLLISIONS AT $\sqrt{s} = 1.8$ TEV

Gerald C. Blazey
(for the DØ Collaboration)
Fermi National Accelerator Laboratory
PO Box 500, Batavia, IL 60510, USA

Abstract

We report on preliminary measurements of the central, $|\eta| \leq 0.5$, inclusive jet and dijet cross sections at $\sqrt{s} = 1.8$ TeV. Two data sets with integrated luminosities of 91 pb^{-1} and 14 pb^{-1} were collected at the Fermilab Tevatron $p\bar{p}$ Collider with the DØ detector. The inclusive jet cross section measured with both data sets and reported as a function of transverse jet energy ($35 \text{ GeV} \leq E_T \leq 470 \text{ GeV}$) and the dijet cross section measured with the 91 pb^{-1} data set and reported as a function of dijet mass ($200 \text{ GeV} \leq M_{JJ} \leq 1 \text{ TeV}$) are in excellent agreement with next-to-leading order QCD.

Presented at the XXXIst Rencontres de Moriond
QCD and High Energy Hadronic Interactions
Les Arcs, France, March 23–30, 1996

Introduction

High transverse momentum jets are predominately produced in proton–antiproton collisions by two body scattering of a single proton constituent with an antiproton constituent. Such events typically produce a pair of back–to–back jets (clusters of particles), each resulting from the fragmentation of a final state quark or gluon. Predictions for the inclusive jet cross section have been made using next–to–leading order (NLO) QCD^{1,2,3}. These α_s^3 calculations, which include the possibility of a third radiated parton, reduce theoretical uncertainties to 10–20%. The improvement can be attributed to greater stability of the calculation with respect to the renormalization scale, the use of modern parton distribution functions (pdf), and to improved agreement between jet algorithms at the experimental and theoretical level. We measure the central cross section for jet production as a function of jet energy transverse to the incident beams and the central dijet cross section as a function of dijet mass in the DØ Detector⁴ at the Fermilab Tevatron Collider. Both cross sections, when compared to the NLO predictions, constitute a rigorous test of NLO QCD. Previous measurements of inclusive jet and dijet production with smaller data sets have been performed by the UA2⁵ and CDF⁶ experiments.

Jet and Event Selection

Jet detection in the DØ detector primarily requires the uranium–liquid argon calorimeters which cover pseudorapidity $|\eta| \leq 4.1$ ($\eta = -\ln(\tan(\theta/2))$ where θ is the polar angle of the object relative to the proton beam). The calorimeters have electromagnetic and hadronic single particle resolutions of $15\%/\sqrt{E}$ and $50\%/\sqrt{E}$, respectively. They are transversely segmented into projective towers of $\Delta\eta \times \Delta\phi = 0.1 \times 0.1$ and have longitudinal segmentation of eight to eleven segments depending on η . The electromagnetic modules (EM) include the first four longitudinal segments and the coarse hadronic modules (CH) the final longitudinal segment. The intervening segments comprise the fine hadronic modules and the intercryostat detectors. The total calorimetric depth exceeds seven nuclear interaction lengths for $|\eta| \leq 0.5$. The calorimeters are also segmented into trigger tiles of $\Delta\eta \times \Delta\phi = 0.8 \times 1.6$ and trigger towers of $\Delta\eta \times \Delta\phi = 0.2 \times 0.2$, where ϕ is azimuthal angle. The event vertex is determined using tracks reconstructed in the central tracking system. The detector includes two trigger scintillator hodoscopes located on each side of the interaction region at $1.9 < |\eta| < 4.3$. Timing distributions of particles traversing the two hodoscopes indicate the occurrence of a single inelastic interaction or of multiple inelastic interactions during a single beam–beam crossing.

Event selection occurred in two hardware stages and a final software stage. The initial hardware trigger selected an inelastic particle collision as indicated by the hodoscopes. The

next trigger stage required transverse energy above a preset threshold in the calorimeter trigger tiles for 1994–1995 data and towers for the 1992–1993 data. Selected events were digitized and sent to an array of processors. Jet candidates were then reconstructed with a fast cone algorithm and the entire event logged to tape if any jet E_T exceeded a specified threshold. During the 1994–1995 (1992–1993) data run, the software jet thresholds were 30, 50, 85, and 115 (20, 30, 50, 85, 115) GeV with integrated luminosities of 0.355, 4.56, 51.7 and 90.7 (0.00950, 0.0774, 1.02, 7.95, and 13.7) pb^{-1} , respectively. To avoid saturating the data acquisition bandwidth, only a fraction of the lower threshold triggers was accepted.

Jets are reconstructed offline using an iterative jet cone algorithm with a cone radius of $\mathcal{R}=0.7$ in η - ϕ space ⁷⁾. The algorithm uses preclusters formed from 1 GeV seed towers. The jet E_T is defined as the sum of each cell E_T within the cone. The E_T -weighted rapidity and azimuth of the jet are calculated and the center of the cone repositioned on this axis. The jet E_T and direction are then recalculated until the cone direction is stable. The final jet directions are calculated using the components of the jet energy vector. After all jets are formed, closely spaced jets which share more than 50% of the smaller jet energy are merged; otherwise, the energy is split evenly between the two, and the directions accordingly recalculated. For the 1994–1995 data, prior to reconstruction, isolated energetic cells (mainly due to calorimeter noise) were removed from the event. Removal occurred for 3% of 100 GeV jets and for 10% of 350 GeV jets. Any removed cell located within $\mathcal{R}=0.7$ of a jet axis was restored to the jet if the cell had no more than 50% of the final, restored jet energy. The restored jet rapidity was recalculated with the E_T weighted rapidity of the jet and restored cell.

Background jets from isolated noisy calorimeter cells and accelerator losses are eliminated with quality cuts. The fraction of energy detected in the EM modules for any jet must lie between 5 and 95%. Also the ratio of energy in the second most energetic cell in a jet to the most energetic cell must be greater than 0.10 (this cut is not imposed on jets which include restored cells). Background from the Main Ring accelerator passing through the CH modules is eliminated by requiring that the fraction of energy in the CH modules be less than 40%. Background from cosmic ray bremsstrahlung is eliminated by requiring the magnitude of the summed transverse energy in an event, \cancel{E}_T , to be less than 70% of the leading jet E_T . Residual contamination from the backgrounds is estimated to be less than 2% at all $E_T < 500$ GeV based on Monte-Carlo simulations and scanning of all very high jet E_T candidates ⁸⁾. The overall jet selection efficiency for $|\eta| \leq 0.5$ has been measured as a function of jet E_T and found to be $97 \pm 1\%$ below 250 GeV and $94 \pm 1\%$ at 400 GeV.

At high instantaneous luminosity more than one interaction in a single beam crossing is probable. The event reconstruction retains, at most, two vertices. The quantity $\mathcal{H}_T =$

$|\sum_{\text{jets}} \vec{E}_T^{\text{jet}}|$ was calculated for both vertices. Except for soft radiation falling below the jet reconstruction threshold of 8 GeV, $\mathcal{H}_T = \cancel{E}_T$. The vertex with the minimum \mathcal{H}_T is selected as the event vertex and used to calculate jet E_T and η . This reduced the cross section by 5% at 100 GeV and 10% at 300 GeV. This procedure is not required for the 1992–1993 data set as the instantaneous luminosity was relatively low. The selected vertex is also required to be within 50 cm of the detector center. The z requirement is $90 \pm 1\%$ efficient, independent of E_T .

Energy Calibration and Resolution Unsmearing

The transverse energy of each jet has been corrected for offsets, O , due to underlying events and noise/zero suppression; the fraction of particle energy showering, S , outside the jet cone; and calorimeter hadronic energy response, R . The corrected jet energy, E_{jet} , can be related to the measured energy, E_{meas} , by $E_{\text{jet}} = [E_{\text{meas}} - O]/[(1 - S) * R]$. The offsets, O , to jet energy are extracted from the energy densities as a function of η for single and double minimum bias events. The single interaction energy deposition is due to a single underlying event and to noise/zero suppression ($U+N$). The double interaction deposition is due to *two* underlying events and the noise/zero suppression ($2U+N$). The η dependent functions U and N are then used to subtract the energy offsets on a jet-by-jet basis. The underlying interaction correction for each jet is determined by the average number of interactions expected for the instantaneous luminosity observed at the time the jet was recorded.

The out-of-cone showering correction, S , should compensate for energy (from particles emitted within the cone) that leaks outside the cone during calorimeter showering. This puts the experimental measure of jet energy on identical footing as the theoretical NLO treatment which includes parton radiation inside the cone. Similarly, S must compensate for particles emitted outside the cone but which deposit some energy inside. The energy spectrum for jets was simulated with HERWIG and the pattern of energy deposition at the cell level for each particle taken from a sample of single particle showers collected at a test beam ⁴⁾. After reconstruction with the 0.7 cone algorithm and for jets in the central unit of rapidity, no net energy flow was measured across the jet cone boundary.

The response correction, R , is based on the E_T balance of the photon and jets, after the jets are corrected for offset, in a photon-jets event sample. The photon candidates, designated “ γ ”, include direct photons and photon-like jets that have fragmented into photons. The response of the calorimeter to electrons is linear to $\leq 1\%$ for energies above 10 GeV ⁹⁾. The absolute electromagnetic calibration is determined using dielectron and diphoton decays of the Z , J/ψ , and π^0 resonances ¹⁰⁾. The “ γ ” candidates are selected by requiring a reconstructed

electromagnetic deposition above 8 GeV, candidate isolation, and shower shape consistent with that of a test beam electron ⁹⁾. The latter two requirements ensure that these “ γ ” candidates have electromagnetic response, whether they are photons or photon-like jets. The hadronic response for “ γ ”-jet events can be derived from data using the conservation of momentum: $R = 1 + [n_{T\gamma} \cdot \hat{E}_T] / E_{T\gamma}$, where $n_{T\gamma}$ and $E_{T\gamma}$ are the transverse direction vector and energy of the γ and \hat{E}_T is the missing E_T vector. Figure 1 shows the measured hadronic response, R , as a function of $E' = E_{T\gamma} \cdot \cosh(\eta_{\text{jet}})$, the expected jet energy if all the hadronic energy were contained in a single jet at the leading jet rapidity η_{jet} . The most energetic jets are located in the forward calorimeter. A 3% response correction between the central and forward calorimetry was included, determined by direct comparison of the response of equal energy jets in the two regions. Figure 1 also shows the measured leading jet energy, E_{meas} , as a function of E' . Together, the two curves provide the relationship between E_{meas} and R .

The response, R , is directly measured with data for E_{meas} less than 350 GeV and is extended to higher energies using full GEANT simulated γ -jet events. The simulated jet response is in good agreement with the data for E_{meas} less than 350 GeV. Statistical errors on the response function are 2% at 100 GeV and 4% at 300 GeV. Figure 2 shows the mean total jet correction as a function of E_T for $|\eta| \leq 0.5$. The upper and lower curves represent the correction uncertainty. Errors due to additional soft radiation in the event and statistical errors from the high E_T simulation have been included.

The jet energy scale corrects only the average response of a jet, so the steeply falling jet spectrum is distorted by jet energy resolution and to a negligible extent by the η resolution. The observed E_T spectrum is corrected for resolution smearing by assuming a trial unsmeared spectrum, $(AE_T^{-B}) \cdot (1 - 2E_T/\sqrt{s})^C$, smearing it with the measured resolution, and comparing the smeared result with the measured cross section. This procedure is repeated by varying the parameters A , B , and C until the observed cross section and smeared trial spectrum are in good agreement. At all E_T the resolution, as measured with dijet E_T balance, is well described by a gaussian distribution; the variance at 100 GeV is $6.5 \pm 1.5\%$. The resolution has been corrected for additional soft radiation and smearing caused by particles radiated initially outside the reconstruction cone. The resolution errors include contributions from the soft radiation correction uncertainties and differences between simulated resolution and the data. The correction reduces the observed cross section by $20 \pm 5\%$ ($10 \pm 5\%$) at 60 GeV (400 GeV). The smearing correction errors have been estimated by varying the resolution function within errors, performing the procedure on distributions obtained from JETRAD NLO predictions using various pdfs ¹⁾, and using non-gaussian distributions for the jet resolution.

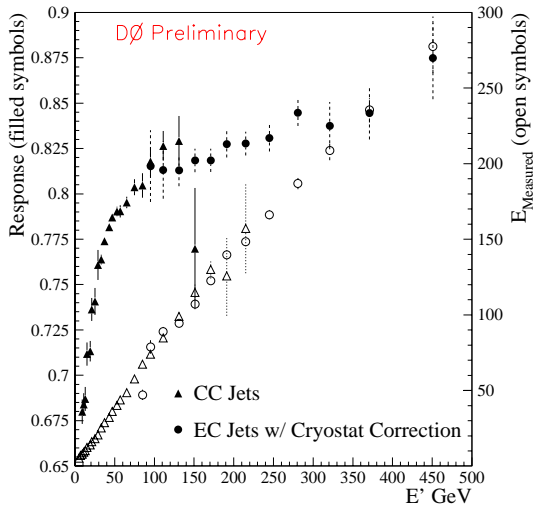


Figure 1: Jet response (left axis, filled symbols) and measured jet response (right axis, open symbols) versus E_T . Data from the central (triangles) and end calorimeters (circles) are included.

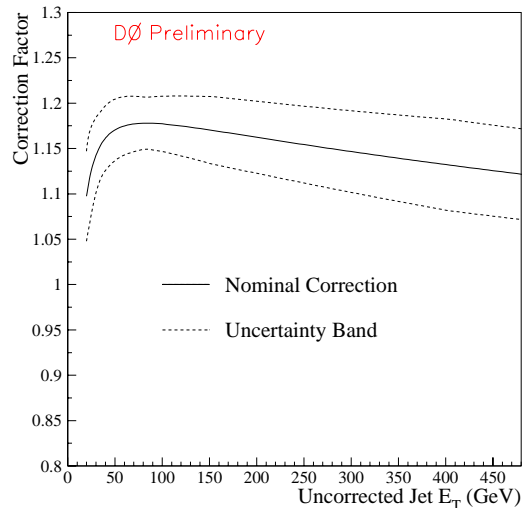


Figure 2: The jet energy scale correction factor as a function of uncorrected jet energy. The upper and lower curves represent the total uncertainty.

Preliminary Results

The inclusive jet cross sections are computed in contiguous E_T ranges from the individual trigger sets. The relative normalizations of the four 1994–1995 sets are established by requiring equal cross-sections in the regions where two trigger sets overlap and are efficient. The adjustments are $2.8 \pm 1.3\%$, $5.7 \pm 1.5\%$, and $6.3 \pm 1.6\%$ for the three highest E_T trigger sets. The final observed cross section corrected for jet and event selection efficiency, shown in Fig. 3, includes data from the lowest E_T trigger in the range 50–90 GeV, from the next trigger in the range 90–130 GeV, then 130–170 GeV, and above 170 GeV from the highest E_T trigger. The errors are statistical only. There is an overall luminosity error of 8%. The same procedure was performed on the 1992–1993 data set. The E_T values plotted are the mean value of the E_T bin center and the average jet E_T in the bin. The statistical errors are uncorrelated from point to point. The inset shows the total systematic error (without the luminosity error) as a function of E_T which is dominated by the energy scale uncertainty.

Comparison to NLO

Figure 3 also shows a prediction for the inclusive jet cross section from the NLO parton event generator JETRAD¹⁾. Note the good agreement over seven orders of magnitude. The data and theoretical calculation are binned identically in E_T . The NLO calculation requires

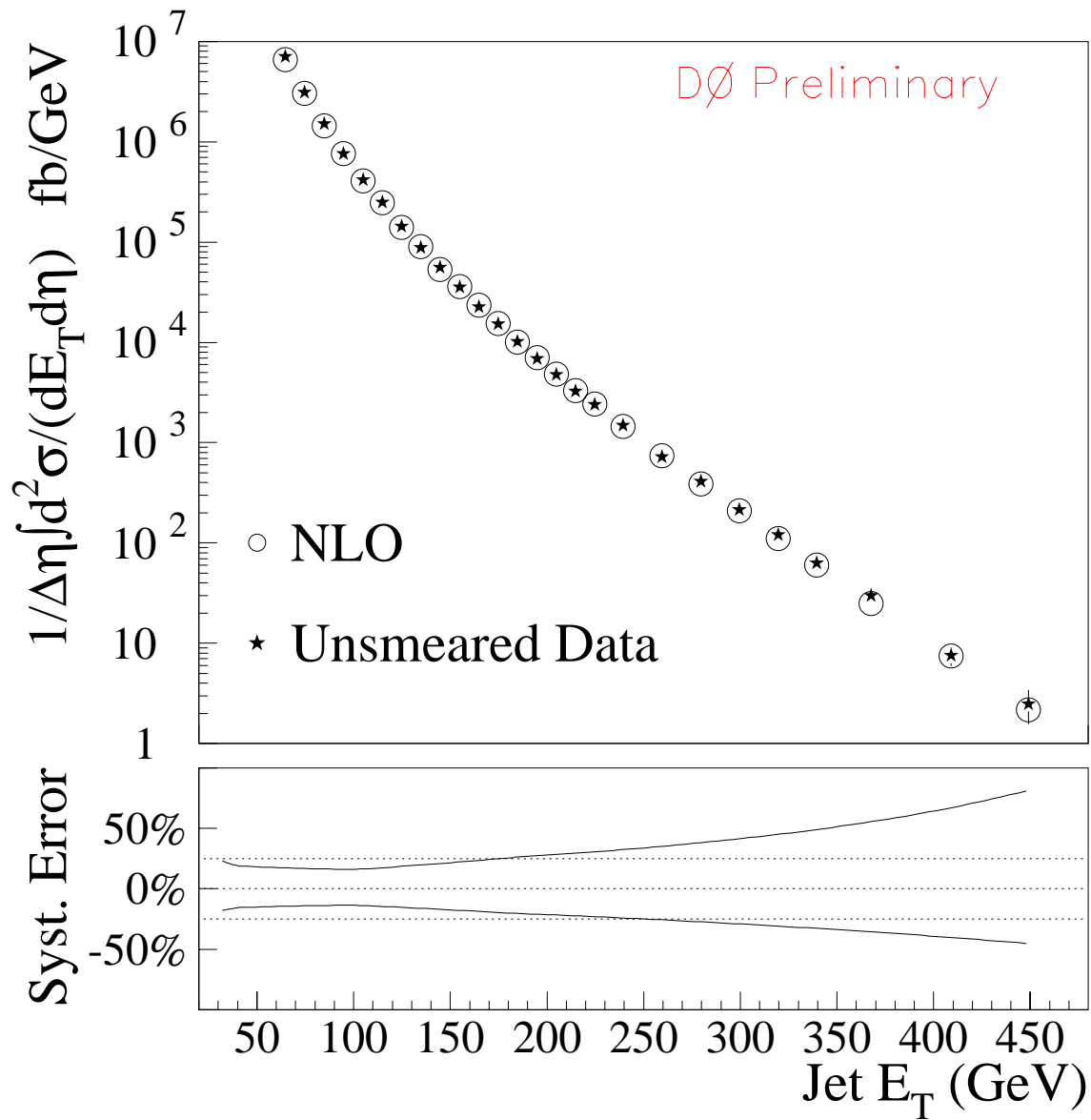


Figure 3: A comparison of the central inclusive cross section to a NLO calculation. The points include statistical errors. The inset curves represent plus and minus 1σ systematic error.

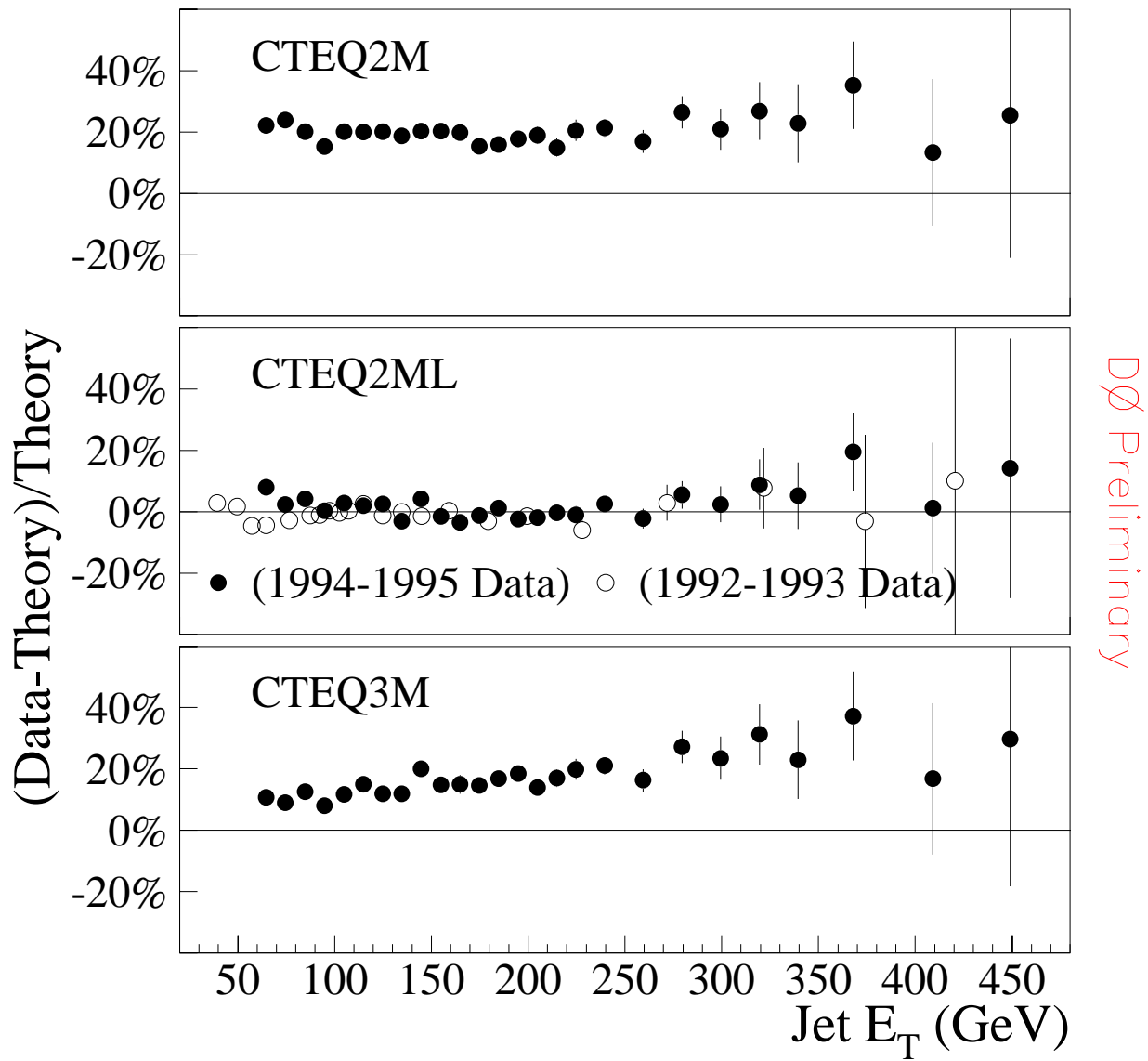


Figure 4: Difference between the data and three QCD predictions normalized to the theoretical prediction $((D - T)/T)$. The solid (open) symbols are for the 1994–1995 (1992–1993) data.

specification of the renormalization scale ($\mu = E_T/2$ where E_T is the maximum jet E_T in the generated event), parton distribution function (CTEQ2ML¹¹), and the parton clustering algorithm. Partons within $1.2 \mathcal{R}$ of one another were clustered if they were also within $\mathcal{R}=0.7$ of their E_T weighted η, ϕ centroid. The value of $1.2 \mathcal{R}$ was determined by overlaying jets from separate events and determining the separation at which the jet reconstruction algorithm could resolve the individual jets. Variation of the pdf can alter the prediction 10-20% depending on E_T . Variation of μ between $0.25E_T$ and $2E_T$ can alter the theoretical normalization by $\sim 10\%$. Above 50 GeV the choice of parton clustering between $1.2 \mathcal{R}$ and $2.0 \mathcal{R}$ alters the normalization by $\sim 5\%$ with a small (2-3%) E_T dependence.

Figure 4 shows the ratio, $(D - T)/T$, for the data (D) and NLO theoretical (T) predictions based on the CTEQ2M, CTEQ2ML, and CTEQ3M pdf's¹¹). The CTEQ2M and CTEQ2ML pdf's are derived from fixed lower energy inelastic scattering data and from HERA ep data. The shapes of both the CTEQ2M and CTEQ2ML predictions are in excellent agreement with the data, as is the CTEQ2ML normalization. The CTEQ2ML pdf was derived by imposing the LEP value of α_s during the pdf derivation. The 1992-1993 data, also shown in the central figure, are in excellent agreement with the 1994-1995 data and the CTEQ2ML prediction. The CTEQ3M pdf includes the deep inelastic and recent HERA data as well as recent W boson asymmetry and Drell-Yan measurements.

The dijet cross section as a function of dijet mass, M_{JJ} , has been determined with the same data sample and the same jet and event selection criteria as the inclusive jet cross section. The dijet mass, $M_{JJ}^2 = 2E_{T1}E_{T2}(\cosh(\eta_1 - \eta_2) - \cos(\phi_1 - \phi_2))$ was calculated with the leading two E_T jets restricted to $|\eta| \leq 0.5$. The mass spectrum has not been corrected for jet resolution. The linear difference between the data and a NLO prediction is shown in Fig. 5. The prediction was calculated with the event generator JETRAD by smearing the energy of the individual jets with the measured jet resolution. The prediction, in excellent agreement with the data between 200 GeV and 1 TeV, incorporates $\mu = E_T/2$, pdf = CTEQ2ML, and parton clustering with a maximum separation of $1.3 \mathcal{R}$. The cross section decreases nearly five orders of magnitude between 200 GeV and 1 TeV. Total systematic errors are indicated by the upper and lower curves.

In conclusion, we have measured the inclusive jet cross section for $|\eta| \leq 0.5$ and $35 \text{ GeV} \leq E_T \leq 470 \text{ GeV}$ and the dijet mass spectrum for $|\eta| \leq 0.5$ and $200 \text{ GeV} \leq M_{JJ} \leq 1 \text{ TeV}$. The QCD NLO model, incorporating modern pdf's, is in excellent agreement with the E_T - dependent shape of the observed central inclusive jet cross section and within experimental and theoretical uncertainties agrees well in absolute normalization. The model is also in agreement with the dijet mass spectrum.

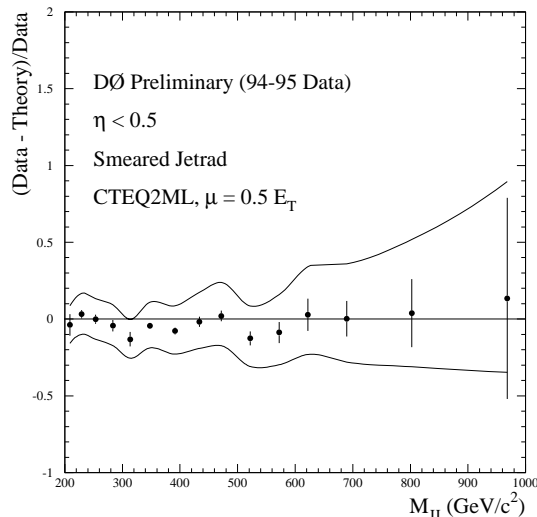


Figure 5: Difference between the dijet cross section as a function of dijet mass and a QCD prediction normalized to the theoretical prediction $((D - T)/T)$.

We thank W. Giele, E. Glover, and D. Kosower for their helpful comments and suggestions. We thank the Fermilab Accelerator, Computing, and Research Divisions, and the support staffs at the collaborating institutions for their contributions to the success of this work. We also acknowledge the support of the U.S. Department of Energy, the U.S. National Science Foundation, the Commissariat à L’Energie Atomique in France, the Ministry for Atomic Energy and the Ministry of Science and Technology Policy in Russia, CNPq in Brazil, the Departments of Atomic Energy and Science and Education in India, Colciencias in Colombia, CONACyT in Mexico, the Ministry of Education, Research Foundation and KOSEF in Korea, CONICET and UBACYT in Argentina, and the A.P. Sloan Foundation.

References

- (1) W. T. Giele, E. W. N. Glover, and D. A. Kosower, Phys. Rev. Letters **73**, 2019 (1994) and private communication. We use the program JETRAD written by these authors.
- (2) S. D. Ellis, Z. Kunszt, and D. E. Soper, Phys. Rev. Letters **64**, 2121 (1990).
- (3) F. Aversa, *et al.*, Phys. Rev. Letters **65**, (1990)
- (4) S. Abachi *et al.*, (DØ Collaboration), Nucl. Instrum. Methods **A338**, 185 (1994).
- (5) J. Alitti *et al.*, (UA2 Collaboration), Phys. Letters **B257**, 232 (1991); Z.Phys.C **49**, 17 (1991).
- (6) F. Abe *et al.*, (CDF Collaboration), Phys. Rev. Letters **70**, 1376 (1993); Phys. Rev. Letters **74**, 3439 (1995); FERMILAB-Pub-96/020-E CDF, Submitted to Phys. Rev. Letters (1996).
- (7) S. Abachi *et al.*, (DØ Collaboration), Phys. Letters **B357**, 500 (1995).

- (8) D. Elvira *et al.*, Ph.D. Thesis, Universidad de Buenos Aires, Buenos Aires, Argentina (1995)
- (9) Jonathan Kotcher for the DØ Collaboration, Proceedings of the 1994 Beijing Calorimetry Symposium, IHEP - Chinese Academy of Sciences, Beijing, China (October, 1994) p. 144.
- (10) P. Renton, “Precision Tests of Electroweak Theories”, Lepton–Photon Conference, Beijing, P.R. China (1995), OUNP–95–20.
- (11) H.L.Lai *et al.*, Phys. Rev. **D51**,4763 (1995)